World Academy of Science, Engineering and Technology
International Journal of Physical and Mathematical Sciences
Vol:2, No:2, 2008

Unsteady Boundary Layer Flow over a Stretching Sheet in a Micropolar Fluid

Roslinda Nazar, Anuar Ishak, and Ioan Pop

Open Science Index, Physical and Mathematical Sciences Vol:2, No:2, 2008 publications.waset.org/11388.pdf

***Abstract*—**Unsteady boundary layer flow of an incompressible micropolar fluid over a stretching sheet when the sheet is stretched in its own plane is studied in this paper. The stretching velocity is assumed to vary linearly with the distance along the sheet. Two equal and opposite forces are impulsively applied along the *x*-axis so that the sheet is stretched, keeping the origin fixed in a micropolar fluid. The transformed unsteady boundary layer equations are solved numerically using the Keller-box method for the whole transient from the initial state to final steady-state flow. Numerical results are obtained for the velocity and microrotation distributions as well as the skin friction coefficient for various values of the material parameter *K*. It is found that there is a smooth transition from the small-time solution to the large-time solution.

***Keywords*—**Boundary layer, micropolar fluid, stretching surface, unsteady flow.

I. Introduction

THE fluid dynamics over a stretching surface is important in many practical applications such as extrusion of plastic sheets, paper production, glass blowing, metal spinning and drawing plastic films, to name just a few. The quality of the final product depends on the rate of heat transfer at the stretching surface. Since the pioneering study by Crane [1] who presented an exact analytical solution for the steady two-dimensional stretching of a surface in a quiescent fluid, many authors have considered various aspects of this problem and obtained similarity solutions. Many authors presented some mathematical results, and a good amount of references can be found in the papers by Magyari and Keller [2, 3], Liao and Pop [4], and Nazar *et al.* [5]. The studies carried out in these papers deal only with steady-state flow, but the flow and thermal fields may be unsteady due to either impulsive stretching of the surface or external stream and sudden change in the surface temperature. Kumari *et al.* [6] studied the unsteady free convection flow over a continuous moving vertical surface in an ambient fluid, and Ishak *et al.* [7] investigated theoretically the unsteady mixed convection boundary layer flow and heat transfer due to a stretching vertical surface in a quiescent viscous and incompressible fluid. Further, Pop and Na [8] and Wang *et al.* [9] deal with the unsteady boundary layer flow due to impulsive starting from rest of a stretching sheet in a viscous fluid.

On the other hand, it is well known that the theory of micropolar fluids has generated a lot of interest and many flow problems have been studied. The theory of micropolar fluids, which display the effects of local rotary inertia and couple stresses, can explain the flow behavior in which the classical Newtonian fluids theory is inadequate. Since introduced by Eringen [10,11], several researchers have considered various stretching problems in micropolar fluids including the present authors (see Ishak *et al.* [12,13]). Motivated by the above-mentioned investigations and applications, in this present paper, we investigate the behavior of the boundary layer flow of an incompressible micropolar fluid over a stretching sheet when the sheet is stretched in its own plane. The stretching velocity is assumed to vary linearly with the distance along the sheet. The transformed governing parabolic partial differential equations in two variables are solved numerically using the Keller-box method for some values of the physically governing parameters.

Manuscript received January 31, 2008. This work was supported by the Research University Grant (UKM-GUP-BTT-07-25-174) under the Engineering Mathematics Group, Universiti Kebangsaan Malaysia.

R. Nazar and A. Ishak are with the School of Mathematical Sciences, Universiti Kebangsaan Malaysia, 43600 Bangi, Selangor, Malaysia (corresponding author (Roslinda Nazar) to provide phone: +603-89213371; fax: +603- 89254519; e-mail: rmn72my@yahoo.com, e-mail: anuarishak@yahoo.com).

Ioan Pop is with the Faculty of Mathematics, University of Cluj, R-3400 Cluj, CP 253, Romania (e-mail: pop.ioan@yahoo.co.uk).

II. Problem Formulation and Basic Equations

Consider the flow of an incompressible micropolar fluid in the region $y > 0$ driven by a plane surface located at $y = 0$ with a fixed end at $x = 0$. It is assumed that the surface is stretched in the *x*-direction such that the *x*-component of the velocity varies linearly along it, i.e. $u_w(x) = cx$, where c is an arbitrary constant and $c > 0$. The simplified two-dimensional equations governing the flow in the boundary layer of a steady, laminar and incompressible micropolar fluid are

$$\frac{\partial u}{\partial x} + \frac{\partial v}{\partial y} = 0, \tag{1}$$

$$\frac{\partial u}{\partial t} + u\frac{\partial u}{\partial x} + v\frac{\partial u}{\partial y} = \left(\frac{\mu + \kappa}{\rho}\right)\frac{\partial^2 u}{\partial y^2} + \frac{\kappa}{\rho}\frac{\partial N}{\partial y}, \tag{2}$$

$$\rho j\left(\frac{\partial N}{\partial t} + u\frac{\partial N}{\partial x} + v\frac{\partial N}{\partial y}\right) = \gamma\frac{\partial^2 N}{\partial y^2} - \kappa\left(2N + \frac{\partial u}{\partial y}\right), \tag{3}$$

subject to the initial and boundary conditions

$t \le 0$: $u = v = N = 0$, for any x, y,

Open Science Index, Physical and Mathematical Sciences Vol:2, No:2, 2008 publications.waset.org/11388.pdf

$$t>0:\ v=0,\ u=u_w(x)=cx,\ N=-n\frac{\partial u}{\partial y},\ \text{at}\ y=0, \qquad (4)$$
$$u\to 0\ ,\ N\to 0,\ \text{as}\ y\to\infty,$$

where u and v are the velocity components along the x- and y-axes, respectively, t is time, N is the microrotation or angular velocity whose direction of rotation is in the $x-y$ plane, μ is dynamic viscosity, ρ is density, j is microinertia per unit mass, γ is spin gradient viscosity and κ is vortex viscosity. Further, n is a constant and $0\le n\le 1$. The case $n=0$, which indicates $N=0$ at the wall represents concentrated particle flows in which the microelements close to the wall surface are unable to rotate. This case is also known as the strong concentration of microelements. The case n=1/2 indicates the vanishing of anti-symmetric part of the stress tensor and denotes weak concentration of microelements. The case $n=1$ is used for the modeling of turbulent boundary layer flows. We shall consider here both cases of $n=0$ and n=1/2.

We introduce the new variables

$$\psi=(c\nu)^{1/2}\xi^{1/2}xf(\xi,\eta),\ N=(c/\nu)^{1/2}\xi^{-1/2}cxg(\xi,\eta),$$
$$\eta=(c/\nu)^{1/2}\xi^{-1/2}y,\ \xi=1-e^{-\tau},\ \tau=ct, \qquad (5)$$

where ψ is the stream function defined in the usual way as $u=\partial\psi/\partial y$ and $v=-\partial\psi/\partial x$, and identically satisfy (1). Substituting variables (5) into (2) and (3) gives

$$(1+K)f'''+(1-\xi)\frac{\eta}{2}f''+\xi\left(ff''-f'^2\right)+Kg' = \xi(1-\xi)\frac{\partial f'}{\partial\xi}, \qquad (6)$$

$$\left(1+\frac{K}{2}\right)g''+(1-\xi)\left(\frac{1}{2}g+\frac{\eta}{2}g'\right)+\xi\left(fg'-f'g\right) - K\xi\left(2g+f''\right)=\xi(1-\xi)\frac{\partial g}{\partial\xi}, \qquad (7)$$

where $K=\kappa/\mu$ is the material parameter. Here γ and j are assumed to be given by $\gamma=\left(\mu+\kappa/2\right)j=\mu\left(1+K/2\right)j$ and $j=\nu/c$, respectively. The boundary conditions (4) become

$$f(\xi,0)=0,\ f'(\xi,0)=1,\ g(\xi,0)=-nf''(\xi,0),$$
$$f'(\xi,\infty)=0,\ g(\xi,\infty)=0. \qquad (8)$$

The physical quantity of interest in this problem is the skin friction coefficient C_f, which is defined as

$$C_f=\frac{\tau_w}{\rho u_w^2}, \qquad (9)$$

where τ_w is the skin friction, given by

$$\tau_w=\left[\left(\mu+\kappa\right)\frac{\partial u}{\partial y}+\kappa N\right]_{y=0}. \qquad (10)$$

Using variables (5) in (9) and (10), we obtain

$$C_f\,\mathrm{Re}_x^{1/2}=\xi^{-1/2}\left[1+(1-n)K\right]f''(\xi,0). \qquad (11)$$

Further, we can obtain some particular cases of this problem.

A. Early Unsteady Flow

For early unsteady flow $0<\tau<<1$, we have $\xi\approx 0$, so (6) and (7) reduce in the leading order approximation to

$$(1+K)f'''+\frac{\eta}{2}f''+Kg'=0, \qquad (12)$$

$$\left(1+\frac{K}{2}\right)g''+\frac{\eta}{2}g'+\frac{1}{2}g=0, \qquad (13)$$

and the boundary conditions (8) become

$$f(0)=0,\ f'(0)=1,\ g(0)=-nf''(0),$$
$$f'(\infty)=0,\ g(\infty)=0. \qquad (14)$$

B. Final Steady-State Flow

For this case, $\xi=1$ and (6) and (7) take the following forms:

$$(1+K)f'''+ff''-f'^2+Kg'=0 \qquad (15)$$

$$\left(1+\frac{K}{2}\right)g''+fg'-f'g-K\left(2g+f''\right)=0 \qquad (16)$$

subject to the boundary conditions (14).

III. Results and Discussion

The transformed equations (6) and (7), satisfying the boundary conditions (8) were solved numerically using the Keller box-method as described in the book by Cebeci and Bradshaw [14] for several values of the material parameter K. Numerical results for the skin friction coefficient, the velocity distributions and the microrotation distributions are illustrated in Fig. 1, Figs. 2-5 and Figs. 6-9, respectively, whereas the values of the skin friction coefficient for the final steady-state flow are tabulated in Table I.

TABLE I
VALUES OF THE SKIN FRICTION COEFFICIENT $C_f\,\mathrm{Re}_x^{1/2}$ FOR VARIOUS VALUES OF K AND n WHEN $\xi=1$

$K\setminus n$	0	½
0	-1.0000	-1.0000
1	-1.3679	-1.2247
2	-1.6213	-1.4142
4	-2.0042	-1.7321

Table I presents the values of the skin friction coefficient $C_f\,\mathrm{Re}_x^{1/2}$ when $\xi=1$ (final steady-state flow) for various

values of K and n. It can be seen that the values are negatives for all values of K and n considered in this study. The values of $C_f \operatorname{Re}_x^{1/2}$ are negatives and increase as n increases which means that the absolute values of $C_f \operatorname{Re}_x^{1/2}$ decrease with n. This is not surprising since $n = 0$ represents strong concentration and $n = 1/2$ represents weak concentration of microelements. Also, it can be observed that $C_f \operatorname{Re}_x^{1/2}$ decreases with K for both cases of $n = 0$ and $n = 1/2$.

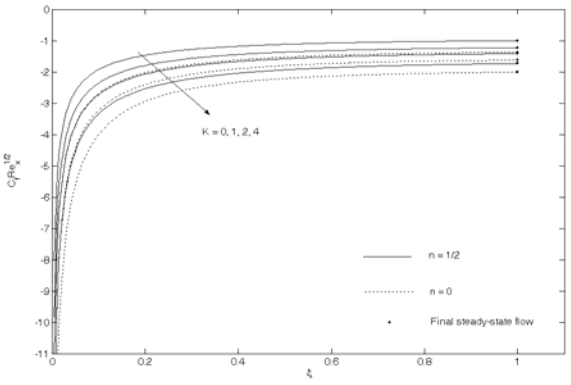

Fig. 1 Variation with ξ of the skin friction coefficient for various K

Fig. 1 represents the variation of the skin friction coefficient $C_f \operatorname{Re}_x^{1/2}$ with ξ. It is noticed that for any fixed n, the values of $C_f \operatorname{Re}_x^{1/2}$ decrease as K increases. It is also found that smaller n produces smaller $C_f \operatorname{Re}_x^{1/2}$. The final steady-state solution $(\xi = 1)$ obtained by solving (15) and (16) are also included in Fig. 1. We notice that there is a very good agreement between the results when we solved the full unsteady boundary layer equations and the final steady-state equations. It is noticed that due to the impulsive motion, the skin friction coefficient has large magnitude (absolute value) for small time ($\tau \approx 0$ or $\xi \approx 0$) after the start of the motion, and it decreases monotonically and reaches the steady-state values at $\xi = 1$ $(\tau \to \infty)$. There is, therefore, a smooth transition from the small-time solution to the large-time solution.

Figs. 2 and 3 show the resulting dimensionless velocity profiles for various values of K with $n = 0$ and $n = 1/2$. Fig. 2 represents the velocity profiles of initial flow $(\xi = 0)$ and early unsteady flow $(0 < \xi << 1)$, while Fig. 3 shows the velocity profiles of final steady-state flow $(\xi = 1)$.

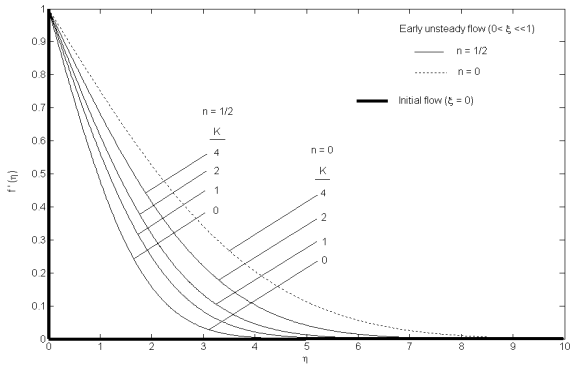

Fig. 2 Velocity distribution of initial flow $(\xi = 0)$ and early unsteady flow $(0 < \xi << 1)$ for various K with $n = 0$ and $n = 1/2$

Both figures show that the velocity boundary layer thickness increases with increasing values of K, for both cases of $n = 0$ and $n = 1/2$. For a particular value of K, the velocity decreases monotonically with η, and becomes zero at the outside of the boundary layer. This property satisfies the boundary condition $f'(\infty) = 0$. Therefore, these figures support the validity of the present results. In Fig. 2, the initial state $(\xi = 0)$ is described by the thick lines on the axes. This rectangular profile is quasi; the "mother" of all the later unsteady profiles.

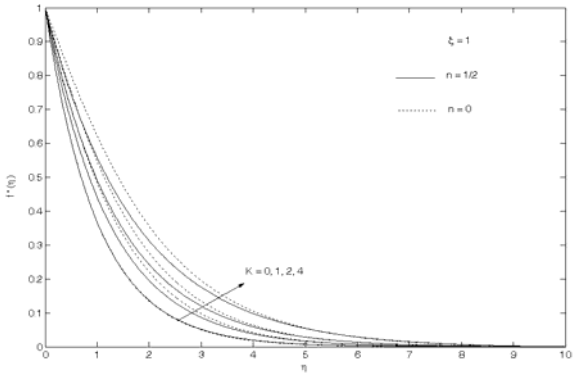

Fig. 3 Velocity distribution of final steady-state flow $(\xi = 1)$ for various K

Figs. 4 and 5 represent the velocity profiles of fully developed unsteady flow and final steady-state flow for the cases $n = 0$ and $n = 1/2$, respectively. These figures show that the velocity profiles corresponding to increasing of ξ $(0 < \xi < 1)$ approach the steady profile corresponding to $\xi = 1$. It can be seen that there is a smooth transition from small time solution $(\xi \approx 0)$ to large time solution $(\xi = 1)$. Again, it is observed that the velocity decreases monotonically with η, and becomes zero far away from the surface, which satisfies the boundary conditions (8).

Open Science Index, Physical and Mathematical Sciences Vol:2, No:2, 2008 publications.waset.org/11388.pdf

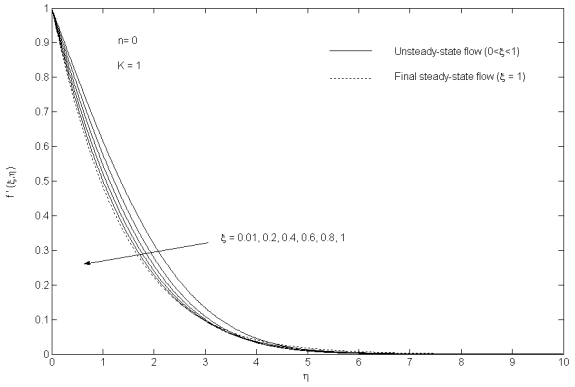

Fig. 4 Velocity distribution of fully developed unsteady flow for various K when $n = 0$

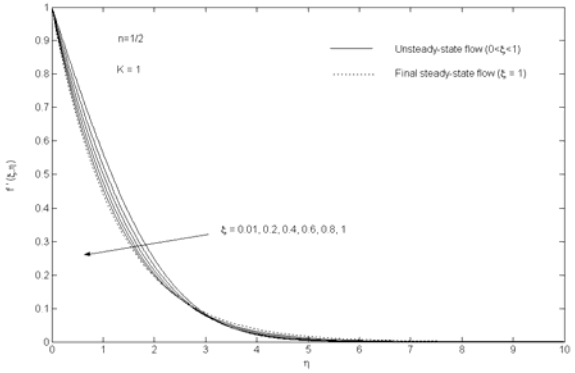

Fig. 5 Velocity distribution of fully developed unsteady flow for various K when $n = 1/2$

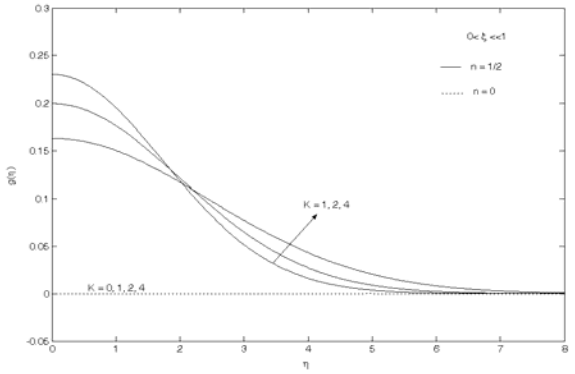

Fig. 6 Microrotation distribution of early unsteady flow $(0 < \xi << 1)$ for various K with $n = 0$ and $n = 1/2$

The microrotation distributions are shown in Figs. 6-9. Fig. 6 shows the microrotation distribution of early unsteady flow $(0 < \xi << 1)$ for various values of the material parameter K with $n = 0$ and $n = 1/2$.

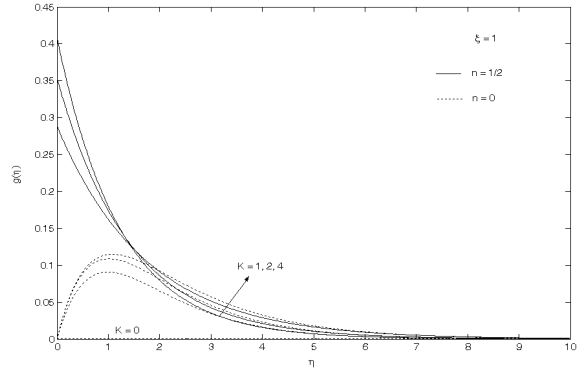

Fig. 7 Microrotation distribution of final steady-state flow $(\xi = 1)$ for various K

When $n = 0$ i.e. the no-spin condition case, for early unsteady flow (Fig. 6), it is found that the value of $g(\eta)$ remains constant, namely zero for all values of the material parameter K, whereas for final steady-state flow, the microrotation shows a parabolic distribution as shown in Fig. 7. When $n = 1/2$, it is observed from both Figs. 6 and 7 that the microrotation continuously decreases with η and becomes zero far away from the plate, which satisfies boundary conditions (14). As expected, the microrotation effect is more dominant near the wall. Also, the microrotation decreases as K increases in the vicinity of the plate but the reverse happens as one moves away from it. It is clear from these figures that the microrotation effects are more pronounced for $n = 1/2$ in comparison to those of $n = 0$.

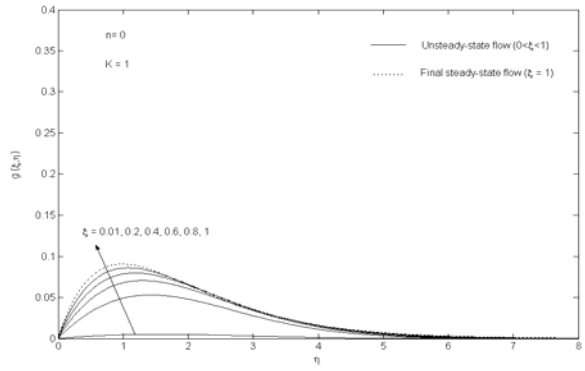

Fig. 8 Microrotation distribution of fully developed unsteady flow for $n = 0$ and $K = 1$

Figs. 8 and 9 represent the microrotation distribution of fully developed unsteady flow when $K = 1$, for $n = 0$ and $n = 1/2$, respectively. From these figures, it is observed that the microrotation profile for $n = 0$ is different as compared to $n = 1/2$. Corresponding to $n = 0$, it has a parabolic distribution whereas for $n = 1/2$, it is continuously decreasing. It is evident from these figures that, there is a smooth transition from small time solution $(\xi \approx 0)$ to large time solution $(\xi = 1)$.

Open Science Index, Physical and Mathematical Sciences Vol:2, No:2, 2008 publications.waset.org/11388.pdf

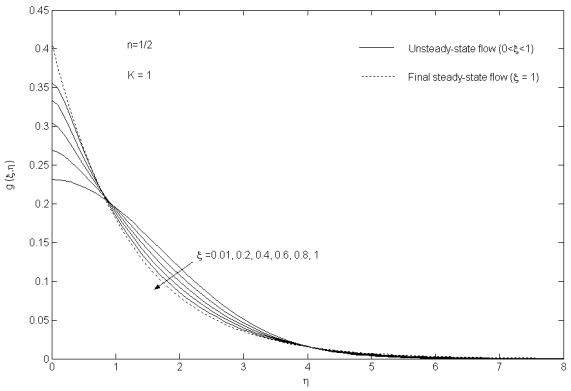

Fig. 9 Microrotation distribution of fully developed unsteady flow for $n = 1/2$ and $K = 1$

REFERENCES

[1] L. J. Crane, "Flow past a stretching plane", *J. Appl. Math. Phys. (ZAMP)*, vol. 21, pp. 645-647, 1970.

[2] E. Magyari, and B. Keller, "Heat and mass transfer in the boundary layers on an exponentially stretching continuous surface", *J. Phys. D: Appl. Phys.*, vol. 32, pp. 577-586, 1999.

[3] E. Magyari, and B. Keller, "Exact solutions for self-similar boundary-layer flows induced by permeable stretching surfaces", *Eur. J. Mech. B-Fluids*, vol. 19, pp. 109-122, 2000.

[4] S. J. Liao, and I. Pop, "Explicit analytic solution for similarity boundary layer equations", *Int. J. Heat Mass Transfer*, vol. 47, pp. 75-85, 2004.

[5] R. Nazar, N. Amin and I. Pop, "Unsteady boundary layer flow due to a stretching surface in a rotating fluid", *Mech. Res. Comm.*, vol. 31, pp. 121-128, 2004.

[6] M. Kumari, A. Slaouti, H. S. Takhar, S. Nakamura, and G. Nath, "Unsteady free convection flow over a continuous moving vertical surface", *Acta Mechanica*, vol. 116, pp. 75-82, 1996.

[7] A. Ishak, R. Nazar, and I. Pop, "Unsteady mixed convection boundary layer flow due to a stretching vertical surface", *Arabian J. Sci. Engng.*, vol. 31, pp. 165-182, 2006.

[8] I. Pop, and T. Y. Na, "Unsteady flow past a stretching sheet", *Mech. Res. Comm.*, vol. 23, pp. 413-422, 1996.

[9] C. Y. Wang, G. Du, M. Miklavcic, and C. C. Chang, "Impulsive stretching of a surface in a viscous fluid", *SIAM J. Appl. Math.*, vol. 57, pp. 1-14, 1997.

[10] A. C. Eringen, "Theory of micropolar fluids", *J. Math. Mech*., vol. 16, pp. 1–18, 1966.

[11] A. C. Eringen, "Theory of thermomicrofluids", *J. Math. Anal. Appl.*, vol. 38, pp. 480–496, 1972.

[12] A. Ishak, R. Nazar, and I. Pop, "Heat transfer over a stretching surface with variable surface heat flux in micropolar fluids", *Phys. Lett. A, vol.* 372, pp. 559–561, 2008.

[13] A. Ishak, R. Nazar, and I. Pop, "Magnetohydrodynamic stagnation point flow towards a stretching vertical sheet in a micropolar fluid", *Magnetohydrodynamics*, vol. 43(1), pp. 83–97, 2007.

[14] T. Cebeci, and P. Bradshaw, *Physical and Computational Aspects of Convective Heat Transfer*. New York: Springer, 1984, p. 391.

Open Science Index, Physical and Mathematical Sciences Vol:2, No:2, 2008 publications.waset.org/11388.pdf